

ANALYSIS OF IMPACT DATA FROM THE DEBIE (DEBRIS IN-ORBIT EVALUATOR) SENSOR IN POLAR LOW EARTH ORBIT

J.P. Schwanethal, N. McBride, S.F. Green, J.A.M. McDonnell¹ and G. Drolshagen²

¹PSSRI, The Open University, Milton Keynes, U.K., MK7 6AA, Email: J.Schwanethal@open.ac.uk

²ESA/ESTEC, P.O. Box 299, NL-2200 AG Noordwijk

ABSTRACT

The Debris In Orbit Evaluator (DEBIE) is an active dust impact detector; two DEBIE sensors were launched on-board the ESA PROBA satellite in October 2001, into a polar low Earth orbit. The detector uses three independent techniques to provide real time space debris and natural meteoroid impact data. The sensor completed its commissioning phase in July 2002. During the period August 2002 to January 2005 DEBIE was active for almost 50% of the time, and has detected more than 238 dust and debris impacts.

1. INTRODUCTION

The Debris In-orbit Evaluator (DEBIE) was devised in 1996 as a low cost and low resource ‘add-on’ for spacecraft (Leese *et al*, 1996). The concept was for a ‘universal flight opportunity’ dust sensor. The DEBIE flight model is shown in Figure 1. DEBIE has several sensors to allow coincident detection of an impacting particle. A signal from these sensors has the potential to provide information on the mass and speed of the particle (see Figure 2). The front target is made from 6 μm aluminium foil mounted on an aluminium mesh. Sensors in front of, and behind the foil (held at 0 V potential) collect the impact plasma, and sensors mounted on the foil-mesh measure the impact momentum. Plasma grid wires mounted alternately positively and negatively charged (at ± 50 V) in front of the foil measure the charge produced when electrons (measured by the PL1e channel) and ions (PL1i channel) are accelerated towards the wires.

Two piezoelectric crystals (PZT1 and PZT2) are held, with epoxy glue, onto the rear of the mesh. Piezoelectric crystals give signals approximately proportional to mv at low to moderate impact velocities. At higher velocities the signals are affected by an enhancement factor due to extra momentum imparted from the recoil of impact ejecta. Foil penetration is indicated by a signal on the rear plasma channel (PL2e). The number of penetrations leads to a flux at a ballistic limit, F_{max} , of 6 μm .

The DEBIE1 system, consisting of two DEBIE sensors



Figure 1. A DEBIE Sensor Unit Flight Model.

(one ram facing and one starboard facing), is mounted on-board the ESA PROBA (Project for On-Board Autonomy) launched in polar LEO (~ 600 km altitude, $e \sim 0$, $i \sim 98^\circ$) on 22nd October 2001, by the Indian Space Agency Polar Satellite Launch Vehicle.

2. NOISE ENVIRONMENT

The initial data appeared dominated by noise events (false triggers). Figures 3 and 4 show PROBA’s geocentric position (latitude and longitude) for all the events on both SUs in April 2003. Figure 3 shows events for when PROBA is on its South-North traverse (i.e. the half of its orbit centred on the ascending node), which will be referred to as PROBA *ascending*. The remaining half of the orbit will be referred to as PROBA *descending*.

A feature that is immediately apparent in the figures, are the bands of ‘noise’ on SU1 and SU2, and a large gap in the SU2 data when ascending (at -50° to 100° longitude and -60° to -15° latitude), that is filled in with data from Sensor Unit 1 (the approximate position of the South Atlantic Anomaly). The two sensors should

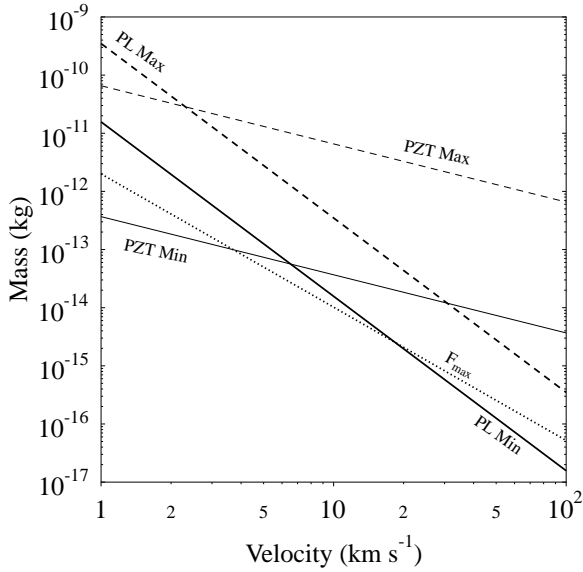


Figure 2. Threshold of Sensor Unit 1 (at FP2 settings). Below approximately 20 km s^{-1} it can be seen that the PL1i threshold (PL Min) is above the F_{max} threshold. Therefore, any impact detected by the PL1i channel, must also have penetrated.

be independent of each other. There are various noise sources, including thermal effects when the spacecraft leaves eclipse and the ascending SU experiences rapid warming. These are visible in Figure 3 at $\sim 55^\circ$ latitude. The false triggering due to the SU entering sunlight is noticeable not just on the momentum sensors, but also on the plasma grid wires. During eclipse, false triggering occurs due to problems with the connection to the PROBA sub-system, an effect which is only a problem when the batteries come online. False triggers also occur due to interactions with the polar cusp regions, and when SU1 is pointed directly at the Sun. The effect of the high levels of noise, is to make the signal voltages on all channels unreliable.

Fortunately there is, however, a way to distinguish a real impact event from the noise, which makes use of the *delay timers*. The delay timers measure the time between the triggering of two channels. We assume a real event will produce delay times similar to those observed during calibration. The first delay (d_1) measures the delay between the PL1e and PL1i triggers, and can have a range of values from $-10 \mu\text{s}$ to $+10 \mu\text{s}$. The second (d_2) and third (d_3) delays measure the times between the PL1e and momentum (PZT) channel, and PL1i and momentum channel triggers respectively. Since the clear false triggers do not contain reasonable values for the delay timers, these events can be automatically filtered, leaving a sub-set of apparently real events. Since the events with real delay values are given a higher ‘quality rating’ than those without, all the ‘real looking’ data are retained, meaning that no impact events are lost.

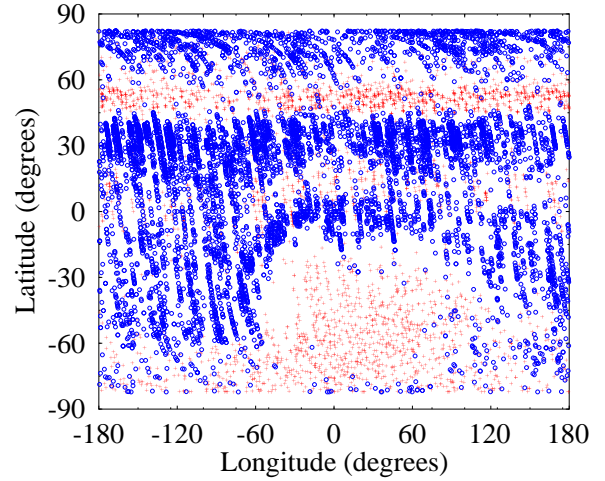


Figure 3. All events during April 2003 when DEBIE is ascending, for Sensor Units 1 (+) and 2 (\circ), when either the plasma channel signal, or momentum channel signal is greater than 100 mV .

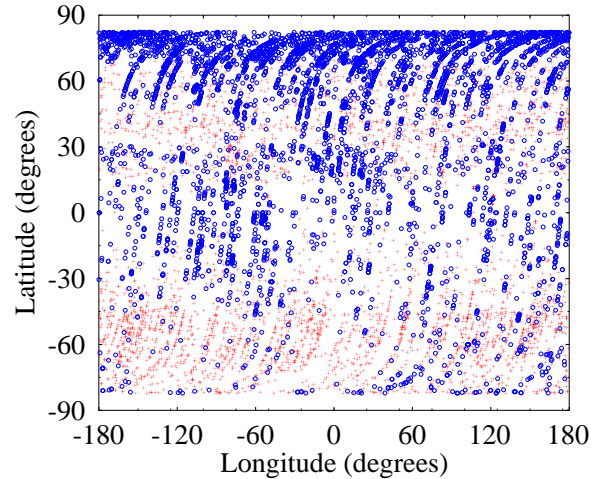


Figure 4. All events during April 2003 when DEBIE is descending for Sensor Units 1 (+) and 2 (\circ), when either the plasma channel signal, or momentum channel signal is greater than 100 mV .

There does, however, remain in the subset of real looking events, a small number of noise events. There are two types of real looking false triggers. The first are due to eclipse line crossings; it is possible that during a thermally induced false trigger, that the two plasma channels trigger within $10 \mu\text{s}$ of each other. This will produce an event filtered as ‘real’. The second type of event is due to excitation of the plasma detection system by the L-Band radar at Eareckson Air Station on Shemya Island. Susceptibility to this L-Band radar is thought to be due to the coincidental match between the radar half-wavelength and the length of the plasma detecting wires on DEBIE (i.e. an aerial effect). These events are easily distinguishable as ‘noise’ events due to PROBA’s geocentric position with respect to either the eclipse line or the radar station

(Figures 5a and b) and are removed by hand leaving a data set of real impact events. The ratio of noise to real impact events is 1000:1.

3. IMPACT FLUXES

During the period August 2002 to February 2005 there were 216 events on SU1 and 25 events on SU2 which produced a signal on PL1i greater than 120 mV (see Table 1). These events are shown in Figures 5a and b (120 mV is a relatively high threshold to adopt, but this is done as it is largely unaffected by the background noise). The total time that the detectors are switched on, is available from the SU housekeeping data; during the period above, SU1 was on for 568.9 days and SU2 for 569.2 days. The impact fluxes at the 120 mV threshold are therefore $13900 \pm 1000 \text{ m}^{-2} \text{ yr}^{-1}$, and $1600 \pm 300 \text{ m}^{-2} \text{ yr}^{-1}$, for SU1 and SU2 respectively. The errors are calculated using counting statistics.

Table 1. Mean fluxes on impacts on DEBIE for August 2002 to February 2005.

Year	On %	Impacts		Flux ($\times 10^3 \text{ m}^{-2} \text{ yr}^{-1}$)	
		SU1	SU2	SU1	SU2
2002	20	27	4	13.5 ± 2.6	2.0 ± 1.0
2003	46	71	10	15.4 ± 1.8	2.2 ± 0.7
2004	82	94	10	11.4 ± 1.2	1.2 ± 0.4
2005	7	24	1	33.3 ± 6.8	1.4 ± 1.4

3.1. Model comparisons

The final fluxes can now be tested against existing models. The MASTER software is multi-platform, and developed by the Aerospace Systems Institute at the Technical University of Braunschweig (TUBS), eta_max space GmbH, and QinetiQ under ESOC contract (Sdunnus *et al.*, 2001). MASTER can predict fluxes for particle diameters larger than $1 \mu\text{m}$.

In order to be able to compare the derived fluxes with those predicted by the models, a particle mass threshold needs to be calculated for the equivalent voltage thresholds of the detector. In this case a PL1i channel threshold voltage of 120 mV has been used. To calculate the threshold mass from the threshold signal voltage, we must assume an impact velocity. MASTER is able to calculate the distribution of debris impact velocities onto PROBA for each spacecraft face, and hence each SU (at the size regime considered, debris is dominant). It would be expected that the ram sensor will see a much higher average impact speed than the starboard sensor. The impact velocities used are $15.0 \pm 2.8 \text{ km s}^{-1}$ for SU1, and $7.5 \pm 1.2 \text{ km s}^{-1}$ for SU2.

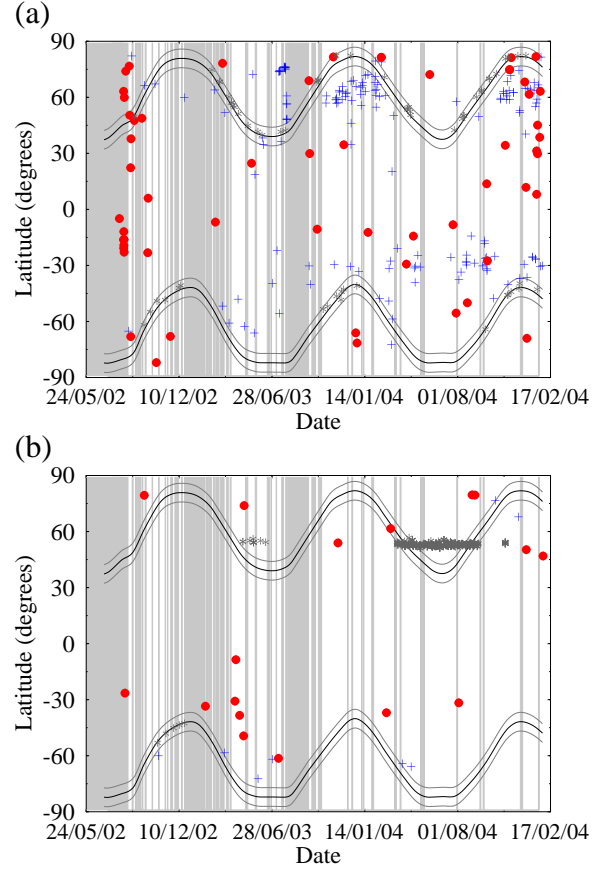


Figure 5. Latitude of events as a function of time for events on (a) SU1 and (b) SU2. Particles impacting when PROBA is ascending are shown as +, and when PROBA is descending are shown as •. The eclipse terminator lines are shown on the graph within a $\pm 5^\circ$ band and are only important for events when PROBA is ascending. '+' events between the two terminator lines are in eclipse. Possible noise events due to crossing the terminator are denoted by *. The off time periods of the SU is shaded, to show when particles could not be detected.

From the DEBIE calibration (Schwanethal, 2004), for SU1,

$$Q_i = \frac{V}{G} = 0.0020 \text{ m v}^{3.0}$$

where, Q_i is the charge collected by the PL1i grid, m is the particle mass, v is the particle velocity, V is the PL1i channel signal voltage, and G is the amplifier gain.

$$G(SU1) = 3.8 \times 10^{12} \text{ VC}^{-1} \quad \text{and}$$

$$G(SU2) = 3.9 \times 10^{12} \text{ VC}^{-1}$$

We thus derive debris threshold masses of

$$m(SU1) = 4.7 \times 10^{-14} \text{ kg} \quad \text{and}$$

$$m(SU2) = 3.7 \times 10^{-14} \text{ kg}$$

If we assume a particle density of 2500 kg m^{-3} , the threshold particle diameters are $1.52 \mu\text{m}$ and $3.03 \mu\text{m}$ for SU1 and SU2 respectively. The ranges of uncertainty (due to the uncertainty in velocity) of the threshold diameter are:

$$\begin{aligned} 1.28 &\leq d_{\text{SU1}} \leq 1.88 \mu\text{m} \\ 2.61 &\leq d_{\text{SU2}} \leq 3.61 \mu\text{m} \end{aligned}$$

The impact fluxes at the threshold diameters are plotted along with the MASTER predictions on Figure 6. It can be seen that the MASTER model under-predicts the fluxes by a factor of 4 on SU1 and 3 on SU2. However, if the trend of the MASTER predictions between $6 \mu\text{m}$ and $100 \mu\text{m}$ were extrapolated below $10 \mu\text{m}$, then this would be consistent with DEBIE impact fluxes.

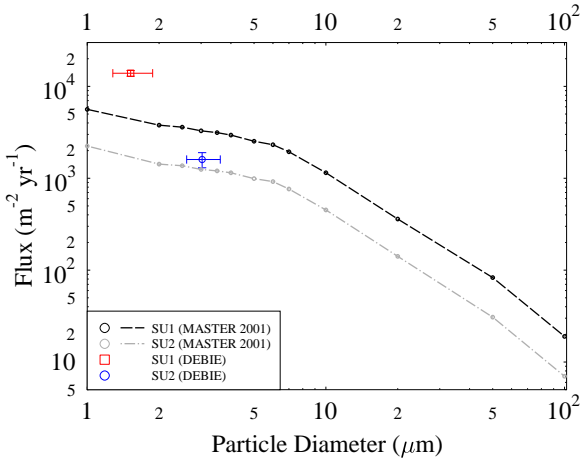


Figure 6. Comparison of the derived DEBIE fluxes, with ESA MASTER 2001.

3.2. LDEF comparison

In 1984, the Long Duration Exposure Facility (LDEF) was placed into a circular low Earth orbit by the Space Shuttle Challenger, at an altitude of 500 km with an inclination of 28.4° . By the time the experiment was retrieved by Columbia in 1990, the orbit had decayed to a little over 300 km, and the satellite had spent about 5.8 years in orbit. PROBA is at a mean altitude of 615 km, and although the two experiments are in differently inclined orbits, the altitudes are similar enough that a comparison can be attempted. This comparison is further aided by the fact that LDEF had 14 faces, and the satellite was gravity gradient stabilised. The East LDEF face was in the direction of the velocity vector; therefore the LDEF East face is directly comparable with DEBIE SU1. The South face of LDEF would then be comparable with SU2 — although due to an offset and tilt of LDEF in orbit, the South face was not exactly perpendicular to the ram direction, and so it is more appropriate to average the North and South faces of LDEF (i.e. port and starboard faces of PROBA).

In previous work, LDEF data have been used with respect to ballistic limit (F_{max}) in aluminium (McDonnell *et al*, 1998, McBride *et al*, 1999). The DEBIE data can also be plotted as in terms of ballistic limit by converting the threshold voltage to F_{max} .

Recalling the McDonnell-Sullivan 1992C Equation (McDonnell & Sullivan, 2001),

$$\frac{F_{max}}{d_p} = 1.272 d_p^{0.056} \left[\frac{\rho_p}{\rho_{Fe}} \right]^{0.476} \left[\frac{\rho_{Al}}{\rho_T} \right]^{0.476} \left[\frac{\sigma_{Al}}{\sigma_T} \right]^{0.134} v^{0.806}$$

Thus for DEBIE, which has an aluminium target,

$$F_{max} = 1.272 d_p^{1.056} \left[\frac{\rho_p}{\rho_{Fe}} \right]^{0.476} v^{0.806} \quad (1)$$

From the calibration of the front ion channel,

$$m = \frac{Q}{0.0020v^3} = \rho V_p = \frac{\pi \rho d_p^3}{6} \quad (2)$$

Therefore,

$$d_p = \sqrt[3]{\frac{6Q}{0.0020v^3 \pi \rho}} \quad (3)$$

Substituting into Eqn. 1, and noting $Q = \frac{V}{G}$,

$$F_{max} = 1.272 \left[\frac{6V}{0.0020v^3 \pi \rho_p G} \right]^{\frac{1.056}{3}} \left[\frac{\rho_p}{\rho_{Fe}} \right]^{0.476} v^{0.806} \quad (4)$$

where V is the signal voltage, G is the gain, ρ_p is the density of the particle, v is the particle velocity, and ρ_{Fe} is the density of iron. Again, we assume the particle density is 2500 kg m^{-3} , and the mean velocity for particles larger than $1 \mu\text{m}$ to be $15.0 \pm 2.8 \text{ km s}^{-1}$ on SU1 and $7.5 \pm 1.2 \text{ km s}^{-1}$ on SU2. Converting the values (using $\rho_{Fe} = 7870 \text{ kg m}^{-3}$) allows the cumulative DEBIE fluxes at the equivalent 'threshold' F_{max} to be plotted with the LDEF data (see Figure 7). It is seen that (as expected) the fluxes at this size regime are dominated by debris, and the DEBIE fluxes are reasonably consistent with those derived from LDEF.

4. DERIVING ORBITS OF IMPACTORS

We have stated that the plasma voltages cannot be directly relied upon for actual charge signal determinations. This has meant that so far, only statistical analysis could be performed on the data. One scenario, however, does allow potential orbit determination — debris clusters. Here, a cluster is defined as a group of events that could be from the same source, and occur at similar positions on subsequent orbits. An event such as an SRM burn will lead to a large number of short lived particles, and in the right conditions it is possible for DEBIE to detect these. Cluster events will always be due to debris

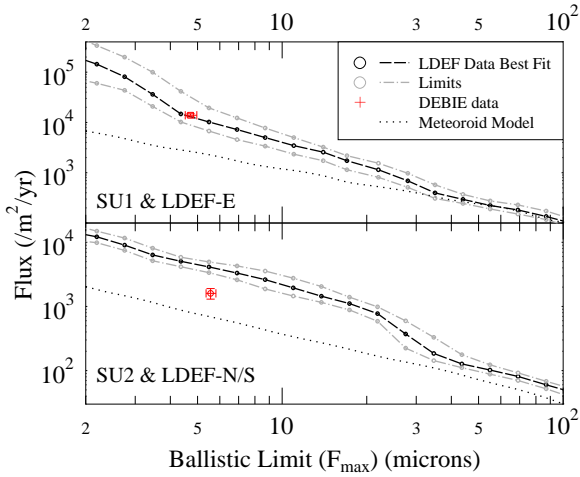


Figure 7. Comparison of the LDEF fluxes (McDonnell *et al*, 2001) with those derived for DEBIE. DEBIE SU1 is equivalent to LDEF East face. DEBIE SU2 is equivalent to LDEF South Face (although to account for LDEF's offset and tilt an average of the LDEF North and South faces is used). The meteoroid model fit refers to the McBride (1998) meteoroid model fit to LDEF

as meteoroids would be unlikely to impact DEBIE at the same latitude on subsequent orbits.

It is then possible to use a programme called ORBELEM (Schwanethal *et al*, 2002), which derives all the possible orbital solutions for an impact, and takes into account the uncertainty in impact speed and direction. If we only consider orbital solutions which are bound to the Earth, then we obtain a distribution of the possible debris orbits which could have been the source of the cluster. Since DEBIE is effectively a flat plate detector, there can be a wide range of impacting orbits. It is possible to better refine the orbit if impacts are detected on both sensor units. Such a case occurred in August 2002; there were a total of six impacts within approximately three days. Five of the impacts were on SU1 and one was on SU2. The events can be seen in context in Figures 5a and b; the events on SU1 (Figure 5a) appear in almost a vertical line between -10° and -30° latitude. The one event on SU2 is shown in a similar position in Figure 5b.

Although there is no direct evidence that these impacts have the same source, given the normal impact rate, it would seem reasonable to assume that these events are not coincidental. For each event the position and velocity information of PROBA can be calculated, along with the pointing direction of both detectors.

There are various outputs from the ORBELEM code that are useful in different circumstances. In the case of cluster events, a unique orbit is expected if all impacts are from the same source. Since the orbit is decaying, this is most likely only useful over a short period. Assuming a fairly consistent orbit over three days, then for each or-

bit the semi-major axis a , eccentricity e and inclination i combination (i.e. as opposed to producing just the eccentricity distribution) can be binned. There are 50 a bins, 10 e bins and 18 i bins leading to 9000 combinations of a , e and i . The values from the seven impacts for each of these bins can be summed. There are 777 bins (out of 9000) which have a probability greater than zero, and of those 238 have a solution for all seven orbits.

Figure 8 shows these results graphically, and shows all the orbital solutions for inclination bins 6 to 9. A 'populated' box in the a versus e 'map' denotes a possible orbit (darker colours represent more probable solutions). The plots show that the orbital solutions are well constrained, with a and e correlated, as would be expected for a common debris source.

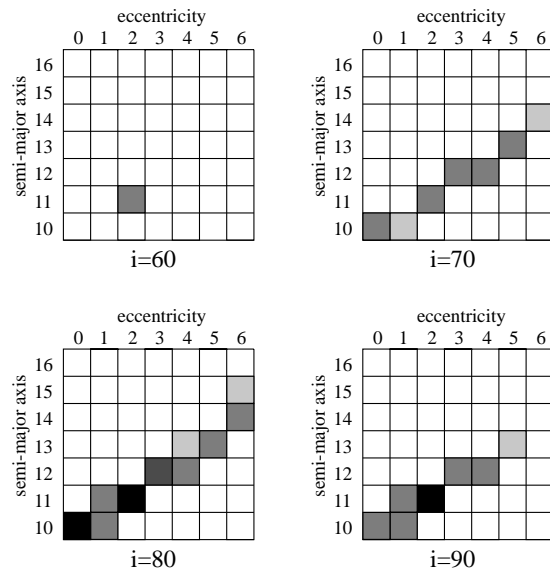


Figure 8. Solutions to the cluster events. The a , e and i combinations are plotted in the form of a semi-major axis versus eccentricity 'map' for various inclination bins. Combinations which are possible show the 'box' filled. The darker the box the higher the probability. It is clear to see that the orbital solution is well constrained, with the most likely orbits in the $i=80$ plot (i.e. an inclination between 80° and 90° , with a low semi-major axis, and low eccentricity). Significant semi-major axis bins (km): $6378 \leq a_{10} < 8029$, $8029 \leq a_{11} < 10108$, $10108 \leq a_{12} < 12726$. Eccentricity bins: $0.0 \leq e_0 < 0.1$, $0.1 \leq e_1 < 0.2$, etc

The majority of the solutions show that the likely source of this cluster of events is a debris 'stream' in a near-polar low eccentricity orbit. It is perhaps counter-intuitive to expect a range of impacts that occur when the detector is between -10° and -30° latitude, to have common impactor inclinations that are polar.

5. CONCLUSIONS

DEBIE has been in polar LEO since October 2001, and has been providing useable impact flux data since August 2002. The DEBIE sensor units suffer from noise triggers, due to both the external space environment, and internal spacecraft effects. However, these ‘noise’ events are identifiable, and can be removed from the data set, providing reliable flux determinations at the 1 to 3 μm size regime. The mean impact fluxes at this threshold is $13900 \pm 1000 \text{ m}^{-2} \text{ yr}^{-1}$, and $1600 \pm 300 \text{ m}^{-2} \text{ yr}^{-1}$, for SU1 and SU2 respectively. The data set is dominated by debris impacts, which is consistent with results from other impact detectors.

REFERENCES

- Leese, M.R., McDonnell, J.A.M., Burchell, M.J., Green, S.F., Jolly, H.S., Ratcliff, P.R., Shaw, H.A., DEBIE - A Low Resource Dust Environment Monitor, *ESA Symposium Proceedings on ‘Space Station Utilisation’*, ESA-SP-385, 1996
- McBride, N., Work Package 9, Technical Note Appendix A: Advanced Meteoroid Modelling, Meteoroid and debris flux and ejecta models, final report for ESA contract 11887/96/NL/JG, 1998
- McBride, N., Green, S.F., McDonnell, J.A.M., Meteoroids and Small Sized Debris in Low Earth Orbit and at 1 AU: Results of Recent Modelling, *Adv. Space Res.*, **23**, 73–82, 1999
- McDonnell, J. A. M., Sullivan, K., Hypervelocity Impacts on Space Detectors: Decoding the Projectile Parameters, In J. McDonnell (Ed.), *Hypervelocity Impacts in Space*, 39–47, Unit for Space Sciences, University of Kent.
- McDonnell, J. A. M., McBride, N., Green, S. F., Ratcliffe, P. R., Gardner, D. J., Griffiths, A.D., Near Earth Environment, In Grün, E., Gustafson, B. Å. S., Dermott, S. F., Fechtig, H (Eds.), *Interplanetary Dust*, Springer, 2001
- Schwanethal J.P., McBride N., Green S.F., Detecting Interplanetary and Interstellar Dust with the DEBIE Sensor, *Proceedings of Asteroids, Comets and Meteors*, ESA-SP-500, 2002
- Schwanethal, J.P., Debris In-Orbit Evaluator (DEBIE) Calibration and Data Analysis, *Ph.D. Thesis, The Open University*, 2004
- Sdunnus, H., Bendisch, J., Klinkrad, H., The ESA MASTER’99 space debris and meteoroid reference model, *Proceedings of the Third European Conference on Space Debris*, ESA-SP-473, 2001